

The origin of molecular hydrogen emission in cooling-flow filaments*

G.J. Ferland^{1,2†}, A.C. Fabian¹, N.A. Hatch³, R.M. Johnstone¹,
R.L. Porter^{1,2}, P. A. M. van Hoof⁴, R.J.R. Williams⁵

¹Institute of Astronomy, University of Cambridge, Madingley Road, Cambridge CB3 0HA

²Department of Physics, University of Kentucky, Lexington, KY 40506, USA

³Leiden Observatory, University of Leiden, P.B. 9513, Leiden 2300 RA, The Netherlands

⁴Royal Observatory of Belgium, Ringlaan 3, 1180 Brussels, Belgium

⁵AWE plc, Aldermaston, Reading RG7 4PR

Received

ABSTRACT

The optical filaments found in many cooling flows in galaxy clusters consist of low density ($\sim 10^3 \text{ cm}^{-3}$) cool ($\sim 10^3 \text{ K}$) gas surrounded by significant amounts of cosmic-ray and magnetic-field energy. Their spectra show anomalously strong low-ionization and molecular emission lines when compared with galactic molecular clouds exposed to ionizing radiation such as the Orion complex. Previous studies have shown that the spectra cannot be produced by O-star photoionization. Here we calculate the physical conditions in dusty gas that is well shielded from external sources of ionizing photons and is energized either by cosmic rays or dissipative MHD waves. Strong molecular hydrogen lines, with relative intensities similar to those observed, are produced. Selection effects introduced by the microphysics produce a correlation between the H_2 line upper level energy and the population temperature. These selection effects allow a purely collisional gas to produce H_2 emission that masquerades as starlight-pumped H_2 but with intensities that are far stronger. This physics may find application to any environment where a broad range of gas densities or heating rates occur.

Key words: galaxies: clusters: general – galaxies: clusters: individual: NGC 1275 – galaxies: clusters: individual: NGC 4696 – intergalactic medium – infrared: galaxies

1 INTRODUCTION

The origin of the optical filaments often found near central regions of massive clusters of galaxies remains mysterious (see Johnstone et al 2007 for a discussion of the extensive literature). The presence of dust and blue light, particularly in the centers of these objects, suggests that star formation has occurred, at least in some regions. Their spectra are quite different from H II regions, which we take as representative of emission from gas near newly-formed stars. Low-ionization optical forbidden lines and near-IR H_2 lines are very strong relative to hydrogen recombination lines. No one model can account for these observations (Johnstone et al 2007).

The combination of Spitzer and ground-based observations allows H_2 lines from a wide range of excitation energies to be studied (Johnstone et al 2007). The resulting H_2 population-excitation diagram shows that the level population temperatures correlate with upper-level energies. The high-excitation lines indicate $T_{\text{pop}} \approx 2000 \text{ K}$, substantially hotter than lines from low-lying levels, with $T_{\text{pop}} \approx 300 \text{ K}$. A similar effect occurs in PDRs near

galactic H II regions due to starlight photoexcitation of higher levels (van Dishoeck 2004). The lines produced by this process are far weaker than is seen in these filaments. Generally, radiation from early-type stars cannot produce extremely strong H_2 lines because the luminosity in the lines is, at most, a small fraction of the stellar luminosity in the $1200 - 912 \text{ \AA}$ range (Sternberg 2005). Other energy sources are needed. Shocks due to stellar outflows are one possibility (Fernandes et al 1997; Jaffe et al 2001; Wilman et al 2002).

At least two sources of energy exist that are unique to the cooling-flow environment. The filaments are surrounded by a mix of hot thermal particles and synchrotron-emitting relativistic particles (Sanders & Fabian 2007). The latter are referred to as cosmic rays here. Additionally, Faraday rotation measures and the long linear geometries suggest that magnetic fields are important (Guidetti et al 2007; Taylor et al 2007).

Here we investigate whether non-radiative heating, produced by cosmic rays or dissipative MHD waves, could produce the observed emission. Both would deposit energy into otherwise well-shielded molecular gas. We consider the cores of the filaments, ignoring complications such as a possible ionized sheath that would be produced by *in situ* star formation or mixing layers (Crawford & Fabian 1992). We show that gas energized by non-

* Contains material © British Crown copyright 2007/MoD

† E-mail: gary@pa.uky.edu

Table 1. H₂ line intensities in a filament in the NGC1275 cooling-flow and the Orion Bar

H ₂ Line	I / I(Pα) flow	I / I(Pα) Orion
0-0 S(1) 17.03 μm	0.65	1×10^{-2}
0-0 S(2) 12.28 μm	0.30	9×10^{-3}
1-0 S(1) 2.121 μm	0.70	6×10^{-3}

radiative heating processes can produce an H₂ spectrum that is very similar to those that are observed.

2 CONDITIONS IN SHIELDED CORES

Table 1 compares H₂ line intensities relative to Pα in the Perseus cooling flow with those in the Orion complex. Intensities for the filaments are taken from Table 8 of (Johnstone et al 2007) while those for the Orion Bar are from Sellgren et al (1990) and Allers et al (2005). The Orion Bar is an H⁺ / H⁰ / H₂ interface viewed roughly edge on. Its successive layers of ionization are displaced on the sky, as shown in Section 8.5 of Osterbrock & Ferland (2006, hereafter AGN3). The separate regions are not spatially resolved in the extragalactic case, so the intensities across the Bar were co-added to create the values listed in Table 1. This procedure is not more accurate than a factor of two. Even so, the differences in the line intensities are dramatic. The H₂ lines are far stronger in the filaments than is found in this prototypical H II region. This suggests that additional energy sources are active in the cooling flow filaments.

Could cosmic rays or extra heating, perhaps due to dissipative MHD waves, produce the strong molecular emission? The environment inside a real filament is likely to have a mix of particle densities and be exposed to a range of cosmic rays, dissipative MHD waves, and possibly starlight. We consider only the cosmic ray and wave heating cases here. We do not address questions such as the transport of cosmic rays into possibly magnetically confined filaments, or the process by which kinetic energy in MHD waves might be converted into thermal energy. Rather we follow the effects of these energy sources on the microphysics of the gas and predict the resulting H₂ line intensities.

We use the development version of the spectral synthesis code Cloudy, last described by Ferland et al (1998). AGN3 discuss much of the physics of the environment with extensive reviews of plasma simulation codes. Our treatment of the H₂ molecule, the focus of this paper, is described in Shaw et al (2005).

Our treatment of cosmic rays is described in Ferland & Mushotzky (1984), Abel et al (2005), Shaw et al (2006) and Shaw et al (2007). In molecular gas a primary cosmic ray will produce a shower of secondary electrons which ionize and excite atoms and molecules. Relatively little of the energy goes into heating the gas (AGN3). Conversely, if the gas is highly ionized then nearly all the cosmic-rays energy will be thermalized and little ionization or excitation occurs.

We also consider an “extra heating” case where thermal energy, perhaps produced by dissipative MHD waves, is injected. This energy, ultimately due to the kinetic energy of a filament, is added to the thermalized kinetic energy of the particles in the material. We assume that the combination of plasma stream instabilities and particle-particle collisional coupling is effective enough in maintaining a Maxwellian distribution for the particle distribution functions that the detail of the energy injection process is unimportant. Ion-neutral drift, where charged particles are coupled to the field

and move relative to neutral particles, might be one source of such heat (Loewenstein & Fabian 1990). The effects are quite different from cosmic rays since the heating has no corresponding direct ionization or internal excitation. Ionization and excitation only occurs when the kinetic temperature becomes high enough to overcome energetic thresholds. Comparing the two cases, at a given kinetic temperature gas energized by cosmic rays will be more highly ionized and excited than the “extra-heating” case.

We parameterize the cosmic ray case by the cosmic-ray density relative to the galactic background value. Background cosmic rays produce an H⁰ ionization rate of $2.5 \times 10^{-17} \text{ s}^{-1}$ in gas with a low electron fraction (Williams et al 1998). The range of relative cosmic ray rates includes the values measured by Sanders & Fabian (2007) and is summarized in Section 3 below. In the “extra heating” case, energy is added to the thermal kinetic energy of the particles at a rate specified in $\text{erg cm}^{-3} \text{ s}^{-1}$. It is not now possible to unambiguously convert a measured magnetic field into a wave dissipation rate (Heiles & Crutcher 2005) so we only show the range of rates with observable effects.

H₂ emission is likely to be produced in shielded cores where any ionizing radiation produced by either star formation or cooling-flow emission has been extinguished by surrounding gas. The $z = 0$ metagalactic background is the radiation field incident upon the cloud. This includes the CMB and the 2005 version of the Haardt & Madau (1996) background with both starburst and quasar continua. This continuum is attenuated by a dusty gas with a total hydrogen column density of 10^{21} cm^{-2} . The extinguished continuum has little effect on the simulations presented below but is included for completeness. For the “extra-heating” case we also include cosmic rays with the galactic background value.

There is no direct measurement of the gas metallicity or dust to gas ratio in the filaments. For simplicity we assume galactic interstellar medium gas-phase abundances and dust (Abel et al 2005). Many of the results presented below do not depend critically on these assumptions. Molecular hydrogen forms on grain surfaces in dusty environments. The rate of formation depends on the grain size distribution, temperature, composition and dust-to-gas ratio, all of which are unknown. We adopt the galactic ISM catalysis rate of $3 \times 10^{-17} \text{ cm}^3 \text{ s}^{-1}$ (Jura 1975).

We are interested in molecular regions that must be well shielded from ionizing radiation. The absorbing column imposed on the metagalactic radiation field ensures that little light shortward of 912 Å penetrates. We further assume “Case B” (AGN3), that resonance lines of H I and H₂ have large optical depths because of this large column density. The result is the Lyman lines do not escape and continuum fluorescent pumping of H I and H₂ resonance lines is not important. Absorption of UV radiation by electronic transitions is the main H₂ destruction process in star-forming regions but will be unimportant in the calculations presented below because of the shielding provided by the large column density.

With these assumptions the free parameters are the hydrogen density n_{H} (cm^{-3}) and the cosmic ray or extra heating rates. Pairs of figures, giving the cosmic ray case as the upper panel and the “extra-heating” case as the lower one, will be shown below. The hydrogen density is the x-axis in all cases.

Figure 1 shows the log of the gas kinetic temperature as a function of these parameters. The temperature is the result of heating and cooling processes. In the cosmic ray case the heating per unit volume is proportional to $r_{\text{CR}} n_{\text{H}}$, where r_{CR} is the primary cosmic ray ionization rate and n_{H} is the hydrogen density. The cooling per unit volume is proportional to the collision rate, or n_{H}^2 . The kinetic temperature, usually increasing with the ratio of heating to cooling,

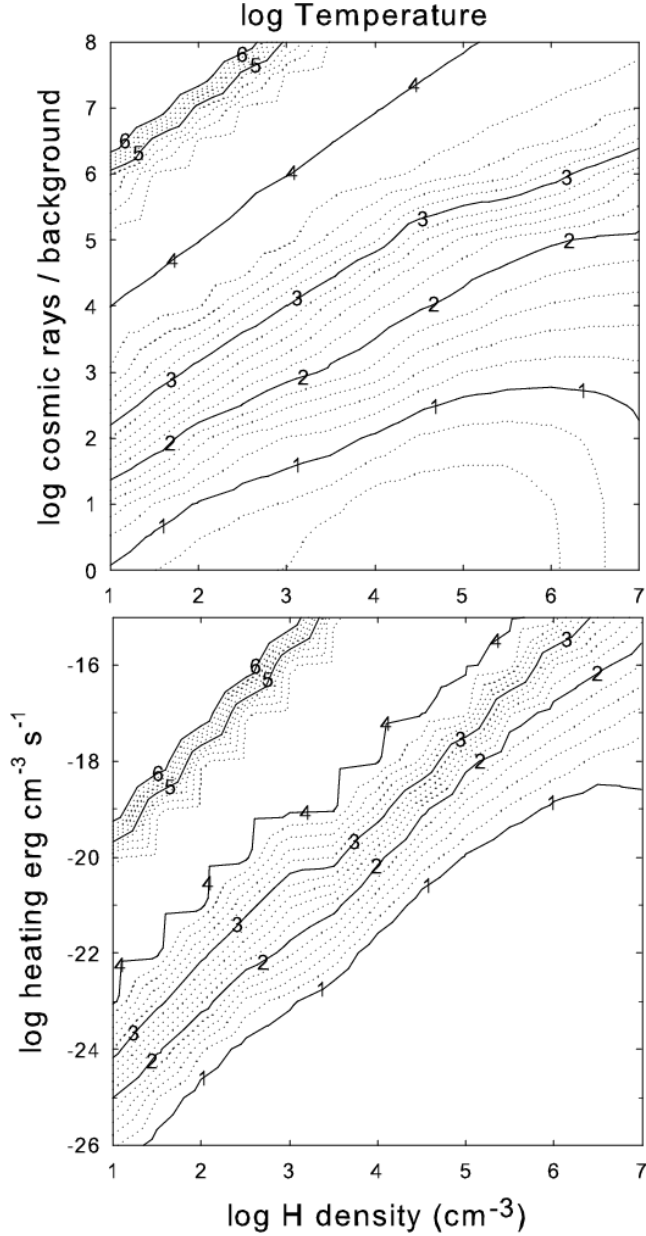


Figure 1. The log of the computed gas kinetic temperature is shown as a function of the hydrogen density and (top) the cosmic ray rate relative to the galactic background and (bottom) the extra heating rate.

is then proportional to $r_{\text{CR}}/n_{\text{H}}$. Lines of constant temperature tend to run at a roughly 45 degree angle corresponding to a constant $r_{\text{CR}}/n_{\text{H}}$ ratio. The curves turn over at the highest densities when collisional cooling is suppressed.

In the “extra-heating” case the heating per unit volume, G_{extra} , is assumed to be independent of density for simplicity. The temperature-determining ratio of heating to cooling is then proportional to $G_{\text{extra}}/n_{\text{H}}^2$. Contours of constant temperature run at a steeper angle as a result.

In both cases the temperatures in the lower right hand corner of Figure 1 are close to the CMB. Temperature increases as the heating increases, reaching the highest values in the upper left corner where the gas is hot and highly ionized.

Figure 2 shows the log of the hydrogen molecular fraction.

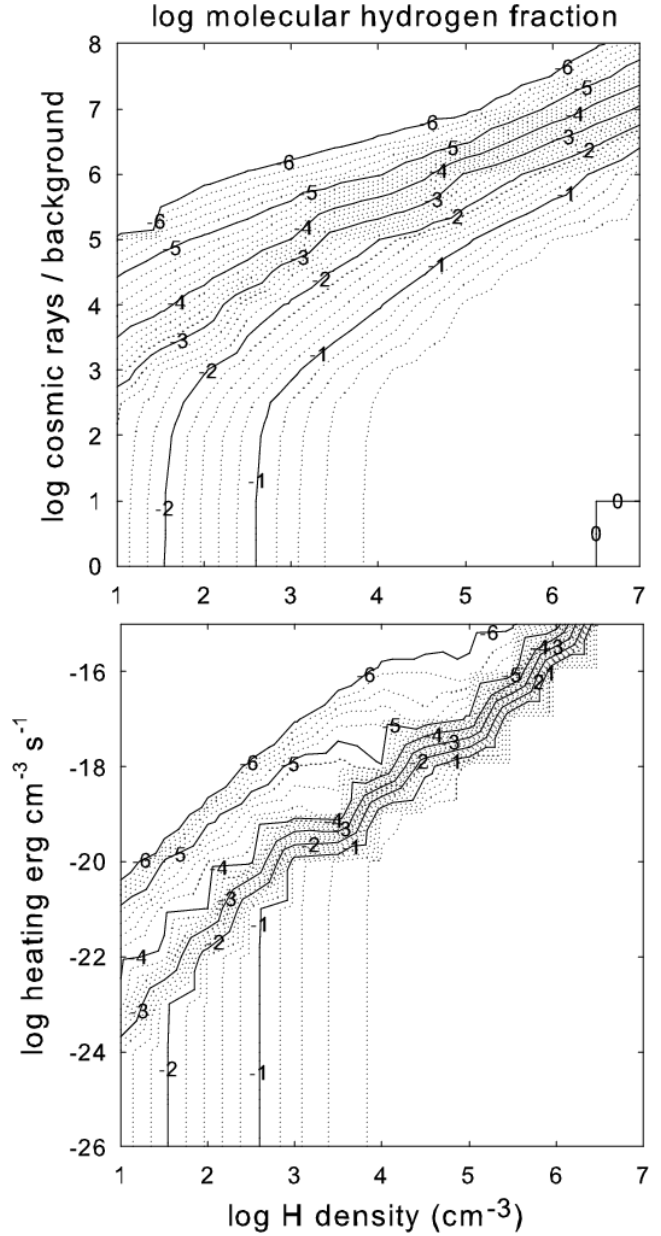


Figure 2. The log of the hydrogen molecular fraction for the cosmic ray (top) and “extra-heating” (bottom) cases.

The lower right corner is predominantly molecular. Gas becomes increasingly dissociated and eventually ionized along a diagonal extending to the upper left. In the cosmic ray case H₂ predominantly dissociates following suprathermal excitation to molecular triplet states. Excitations to the singlets dissociate roughly 10% of the time with the remainder decaying into various levels within the ground electronic state (Sternberg et al 1987; Dalgarno et al 1999). Thus cosmic rays dissociate and excite H₂ even when the kinetic temperature is low. This is in contrast with the “extra-heating” case, where little excitation or dissociation is produced until the kinetic temperature becomes large enough for thermal collisions to drive the processes.

Figure 3 shows the log of the emissivity $4\pi j$ (erg cm⁻³ s⁻¹) of the 1-0 S(1) 2.121 μm line, one of the strongest H₂ lines in the NIR spectrum. The “extra-heating” case is shown to illustrate the effects

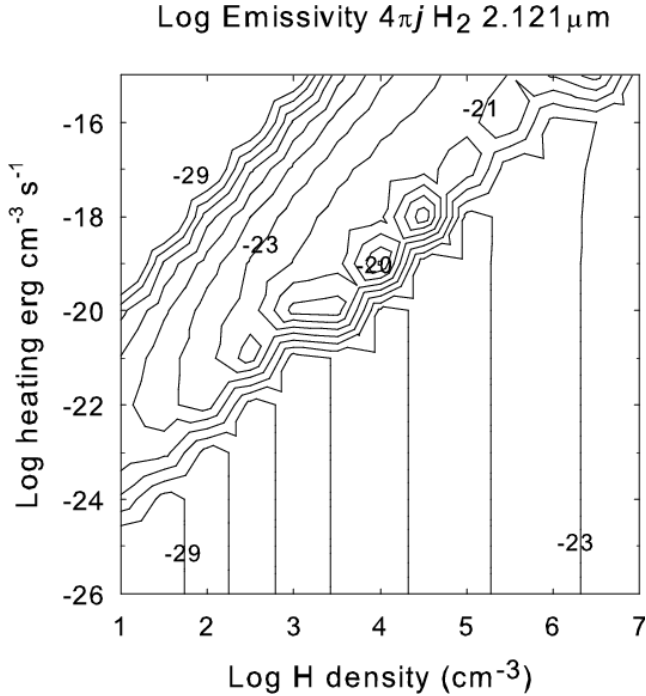


Figure 3. The emissivity of the H₂ 2.121 μm line for the “extra-heating” case. Contours are drawn at 1 dex intervals, ranging from a minimum of $\log 4\pi j$ of -29 up to -20.

of changing temperature. The emissivity is strongly peaked towards a narrow band running along lines of roughly constant temperature and H₂ fraction. Neglecting second-order effects, the emissivity of the line, which is predicted to be collisionally excited, will be proportional to the product of the density $n(\text{H}_2)$ and a Boltzmann factor

$$4\pi j \propto n(\text{H}_2) \exp(-\chi/T) \quad (1)$$

where $\chi \approx 7000$ K is the excitation energy of the upper level of the transition. The gas is mostly molecular in the lower right corner of the diagram but the temperature is too low to excite the transition. The temperature is high in the upper left corner but there is little H₂. The line is emitted efficiently across a narrow band where the product of the H₂ density and Boltzmann factor is large. The ridge of peak emissivity occurs at a gas kinetic temperature of roughly 2000 K.

This result can be generalized. Because of the form of equation 1, a Boltzmann factor that increases exponentially as temperature rises, and an H₂ density that decreases as the temperature increases, the emissivity of a collisionally-excited line will peak when the kinetic temperature is roughly half of the excitation energy. The large changes in emissivity shown in Figure 3 suggest that, if gas exists across the parameter space, a linear detector like a spectrometer will pick out only the peaks. Similar effects are present in emission lines of active galactic nuclei (Baldwin et al 1995).

We now concentrate on the cosmic-ray case since their densities have been measured in regions of the flow (Sanders & Fabian 2007). Figure 4 shows the emissivities, the emission per unit volume ($\text{erg cm}^{-3} \text{s}^{-1}$), of all H₂ lines detected in Johnstone et al (2007). These would be multiplied by the cloud volume, or equivalently the mass of H₂, to obtain line luminosities. We adopt the Johnstone et al (2007) density of $n_{\text{H}} = 10^4 \text{ cm}^{-3}$ and vary the cosmic-ray density. This could occur if gas were trapped in mag-

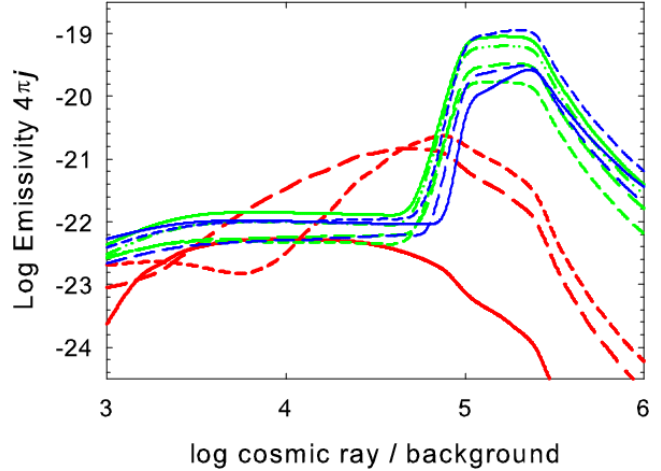


Figure 4. The predicted emissivities of all H₂ lines observed by Johnstone et al (2007) are shown as a function of the cosmic-ray density. The density is $n_{\text{H}} = 10^4 \text{ cm}^{-3}$. The low-excitation rotational lines are (red) 28.21 μm (solid), 17.03 μm (long dash), and 12.28 μm (short dash). The mid-excitation ($2000 \text{ K} < E_U < 8000 \text{ K}$) lines are (green) 2.121 μm (solid), 2.033 μm (long dash), 2.223 μm (short dash), and 2.423 μm (dash dot). High excitation ($E_U > 8000 \text{ K}$) lines are (blue) 1.748 μm (solid), 1.891 μm (long dash), and 1.957 μm (short dash). The emissivity of each line peaks at a temperature that is proportional to its upper level energy, as found by Johnstone et al (2007).

netic field lines, so that n_{H} is constant, but exposed to a range of cosmic ray fluxes, perhaps due to attenuation or shielding. This corresponds to a vertical slice through Figures 1 – 3.

Johnstone et al (2007, Table 11) demonstrate a correlation between a level’s energy and its population temperature T_{pop} , the temperature corresponding to the population distribution. If the levels are thermalized then T_{pop} is the kinetic temperature. Figure 4 shows the predicted emissivities of all lines reported in that paper. If the levels are thermalized then the population temperature will be weighted towards T_{peak} , the kinetic temperature where the emissivity peaks.

The distribution of emissivities shown in Figure 4 reproduces the Johnstone et al (2007) correlation. The observed (T_{pop}) and predicted (T_{peak}) peak temperatures are, for low-excitation levels, $T_{\text{pop}} = 300 \pm 20 \text{ K}$, $T_{\text{peak}} = 610 \pm 450 \text{ K}$, for intermediate excitation, $T_{\text{pop}} = 1730 \pm 250 \text{ K}$, $T_{\text{peak}} = 2300 \pm 400 \text{ K}$, and for high excitation, $T_{\text{pop}} = 2580 \pm 150 \text{ K}$, $T_{\text{peak}} = 2900 \pm 400 \text{ K}$. This agreement, generally within the scatter, is partially fortuitous because the predicted kinetic temperature depends on the gas metallicity, which we simply set to galactic ISM abundances and depletions. The overall trend, where population temperature correlates with excitation temperature, is inescapable for gas with a non-radiative energy source.

3 CONCLUSIONS

The comparison between the relative intensities of H₂ and H I lines in the Orion star-forming region and the cooling-flow filament studied by Johnstone et al (2007) (Table 1) shows that the H₂ lines are far stronger in the filament. Starlight fluorescence produces only weak H₂ emission since only a small portion of the Balmer continuum can be converted into H₂ lines. This strongly suggests that the lines are formed by more efficient, perhaps non-radiative, processes in cooling flows.

Both cosmic rays and dissipative MHD waves are candidates

as extra energy sources. Powerful selection effects introduced by the microphysics cause each emission line to have a peak emissivity at a temperature related to its upper level energy. Both the great strength of the H₂ lines and the observed correlation between excitation potential and population temperature result. Actually, any heating source that simultaneously heats and dissociates H₂ would produce similar effects.

The selection effects cause a collisionally-excited H₂ spectrum to masquerade as classical starlight-induced fluorescence. In the radiative case the lowest-energy levels are collisionally populated and their populations indicate the kinetic temperature. Higher levels are fluorescence excited and have a physically meaningless higher temperature (van Dishoeck 2004). A similar range of population temperatures is produced in the non-radiative cases considered here, but all of the temperatures are real.

The observed cosmic ray densities are large enough to produce the observed emission if n_{H} is lower than usually assumed. Sanders & Fabian (2007) find a cosmic ray energy density of roughly 150 eV cm^{-3} for central regions of the Perseus cluster. For comparison Webber (1998) finds the density of relativistic electrons in the local interstellar medium to be 0.2 eV cm^{-3} . The ratio of cluster to local ISM CR ionization rates, the vertical axis in most of the plots in this paper, is of order 10^3 . The predictions scale roughly as the ratio $r_{\text{CR}}/n_{\text{H}}$. The peak emissivity for high-excitation lines (Figure 4), occurs at $r_{\text{CR}} \approx 10^{5.5}$ for a density of $n_{\text{H}} = 10^4 \text{ cm}^{-3}$. A density of $n_{\text{H}} = 10 \text{ cm}^{-3}$ would have similar spectra at $r_{\text{CR}} \approx 10^3$. Since Johnstone et al (2007) was published, new calculations show that some H₂ collision rates were underestimated by roughly 2 dex (Wrathmall et al 2007). Simple scaling relations suggest that this would lower n_{H} and the gas pressure by a similar amount. This would solve the long-standing puzzle posed by the high gas pressures associated with the high density (Johnstone et al 2007). The filaments' gas pressure would then be in line with the pressure in the surrounding hot plasma.

The emissivities produced by the non-radiative processes we discuss are similar to those assumed by Johnstone et al (2007). Hence the mass of H₂ required to account for the observed emission will be similar. The total mass in warm H₂, roughly $10^5 M_{\odot}$ (Johnstone et al 2007), is a tiny fraction of the mass of cold gas, $\sim 4 \times 10^{10} M_{\odot}$, reported by Salome et al (2006). This suggests that the warm H₂ may be produced in small regions which are affected by the localized deposition of energy in the forms of dissipative MHD waves, cosmic rays, or shocks. We have shown here that such sources of energy can account for the observed spectra.

4 ACKNOWLEDGMENTS

ACF acknowledges support by the Royal Society. RMJ acknowledges support by the Royal Society and STFC. GJF thanks the NSF (AST 0607028), NASA (NNG05GD81G), STScI (HST-AR-10653) and the Spitzer Science Center (20343) for support. PvH acknowledges support from the Belgian Science Policy Office (grant MO/33/017). NAH acknowledges funding from the Royal Netherlands Academy of Arts and Sciences. We thank the referee for a helpful review of the paper.

REFERENCES

Abel, N.P., Ferland, G.J., Shaw, G. & van Hoof, P.A.M. 2005, *ApJS*, 161, 65

- Allers, K. N., Jaffe, D. T., Lacy, J. H., Draine, B. T. & Richter, M. J. 2005, *ApJ*, 630, 368
- Baldwin, J. A., Ferland, G. J., Korista K. T., & Verner, D. 1995, *ApJ*, 455, L119
- Cazaux, S., & Tielens, A.G.G.M., 2002, *ApJ*, 575, L29-L32
- Crawford, C.S., & Fabian, A.C. 1992, *MNRAS*, 259, 265
- Dalgarno, A., Yan, Min, & Liu, Weihong 1999, *ApJS*, 125, 237
- Ferland G.J., Korista K.T., Verner D.A., Ferguson J.W., Kingdon J.B., Verner E.M., 1998, *PASP*, 110, 761
- Ferland, G. J., & Mushotzky, R. F. 1984, *ApJ*, 286, 42
- Fernandes, A.J.L., Brand, P.W.J.L. & Burton, M.G. 1997, *MNRAS*, 290, 216
- Guidetti, D., Murgia, M., Govoni, F., Parma, P., Gregorini, L., de Ruiter, H.R., Cameron, R.A. & Fanti, R. 2007, *A&A*, in press (astro-ph 0709.2652)
- Haardt, Francesco, & Madau, Piero, 1996, *ApJ*, 461, 20
- Heiles, C. & Crutcher, R. 2005, *Magnetic Fields in Diffuse H I and Molecular Clouds*, Chapter in *Cosmic Magnetic Fields*, Edited by Richard Wielebinski and Rainer Beck. Lecture notes in Physics Volume 664
- Jaffe, W., Bremer, M. N., & van der Werf, P. P. 2001, *MNRAS*, 324, 443
- Johnstone, R., Hatch, N., Ferland, G.J., Fabian, A.C., Crawford, C., & Wilman, R. 2007, *MNRAS* in press
- Jura, M., 1975, *ApJ*, 197, 575
- Loewenstein, M. & Fabian, A.C. 1990, *MNRAS*, 242, 120
- Myers, P.C. & Goodman, A.A. 1998, *ApJ*, 326, L27
- Osterbrock D., Ferland G.J., 2006, *Astrophysics of gaseous nebulae and active galactic nuclei*, 2nd. ed. by D.E. Osterbrock and G.J. Ferland. Sausalito, CA: University Science Books,
- Salome, P., Combes, F. Edge, A.C. et al 2006, *A&A*, 454, 437
- Sanders, J.S. & Fabian, A.C. 2007, *MNRAS*, in press (astro-ph 0705.2712)
- Sellgren, K., Tokunaga, A. T., & Nakada, Y. 1990, *ApJ*, 349, 120
- Shaw, G., Ferland, G.J. Abel, N.P. Stancil, P.C. & van Hoof, P.A.M. 2005, *ApJ*, 624, 794
- Shaw, G., Ferland, G. J., Srianand, R., & Abel, N. P. 2006, *ApJ*, 639, 941
- Shaw, G., Ferland, G. J., Srianand, R., Abel, N. P., van Hoof, P. A. M. & Stancil P. C. 2007, *ApJ* in press
- Sternberg, A., 2005, *Astrochemistry: Recent Successes and Current Challenges*, Proceedings of the 231st Symposium of the International Astronomical Union, Edited by Lis, Dariusz C.; Blake, Geoffrey A.; Herbst, Eric. Cambridge: Cambridge University Press, 2005., pp.141-152
- Sternberg, A., Dalgarno, A. & Lepp, S. 1987, *ApJ*, 320, 676
- Taylor, G.B., Fabian, A.C., Bentile, G., Allen, S.W., Crawford, C. & Sanders, J.S. 2007, *MNRAS* in press (astro-ph 0708.3264)
- Tielens, A. G. G. M., 2005, *The Physics and Chemistry of the Interstellar Medium*, Cambridge, UK: Cambridge University Press
- van Dishoeck, E.F. 2004, *ARA&A*, 42, 119
- Webber, W.R. 1998, *ApJ*, 506, 329
- Williams, J.P., Bergin, E.A., Caselli, P., Myers, P.C., & Plume, R. 1998, *ApJ*, 503, 689
- Wilman, R. J., Edge, A. C., Johnstone, R. M., Fabian, A. C., Allen, S. W. & Crawford, C. S. 2002, *MNRAS*, 337, 63
- Wrathmall, S.A., Gusdorf, A., & Flower, D.R. 2007, *MNRAS* 297, 334

This paper has been typeset from a \LaTeX file prepared by the author.